Research Article

Journal of Environmental Nanotechnology

Development of Nanomaterial-incorporated High-performance Lightweight Polyurethane Foam Concrete

P. Manikanta[1*], T. Sreedhar Babu[2] and G. Yesuratnam[3]

[1]Department of Civil Engineering, Jawaharlal Nehru Technological University, Kakinada, AP, India
[2]Department of Civil Engineering, Vasireddy Venkatadri Institute of Technology (VVIT), Nambur, Guntur, AP, India
[3]Department of Civil Engineering and Director IIP and T, Jawaharlal Nehru Technological University, Kakinada, India
Received: 02.02.2026 Accepted: 23.02.2026 Published: 30.03.2026
*saivivekvardhan2@gmail.com

ABSTRACT

Lightweight concrete offers low density and good workability, but is often limited by reduced strength and durability. This study enhances polyurethane foam concrete (PUFC) through the incorporation of nano-alumina (NA), nano-silica (NS), and nano-graphene oxide (NGO) at optimized dosages, resulting in PUFC–NA, PUFC–NS, and PUFC–NGO mixes. Microstructural observations supported the presence and uniform dispersion of nanomaterials within the cementitious matrix. A comprehensive evaluation of rheology, drainage, mechanical strength, shrinkage, and durability was performed. PUFC–NGO achieved a compressive strength of 28 N/mm² at 28 days, compared with 15 N/mm² for the control mix. In addition, both split tensile strength and flexural strength exhibited increases of approximately 50% compared with the control mix, while shrinkage was reduced by about 30%. Chloride ion penetration measured at 90 days showed a reduction of nearly 37%, indicating improved durability. Overall improvements included approximately 35% reduction in shrinkage, 37% reduction in chloride ion penetration, and about 50% enhancement in tensile and flexural strength relative to the control mix. The findings demonstrate that nano-graphene oxide is particularly effective in enhancing the mechanical performance, dimensional stability, and durability of polyurethane foam concrete, thereby improving its suitability for lightweight structural applications.

Keywords: Lightweight concrete (LWC); Polyurethane foam concrete (PUFC); Nano-alumina (NA); Nano-silica (NS); Nano-graphene oxide (NGO).

1. INTRODUCTION

Lightweight concrete (LWC) has gained prominence in recent times because of its lightweight nature, improved workability, reduced dead load, and energy efficiency. Various types of LWCs, such as foam concrete (Qi *et al.* 2024; Turkey *et al.* 2024), fibre-reinforced concrete and nanomaterial-induced concrete are being extensively investigated by various researchers (Tanimola and Efe, 2024). Various foam concretes, such as aircrete (Chen *et al.* 2024), foamcrete (Priyatham *et al.* 2023), geofoam concrete, and perlite foam concrete (Sharook *et al.* 2020) are being increasingly used in the construction industry.

Lightweight concrete comprises several subclasses distinguished by the method used to introduce porosity, among which foam-based systems have gained considerable attention due to their ease of production and uniform pore structure. Within this category, foam concretes produced using chemical or mechanical foaming agents offer greater control over density and workability than aggregate-based lightweight concretes.

Recent investigations over the last decade have examined the incorporation of nanomaterials into polyurethane foam concrete to improve mechanical performance, shrinkage resistance, and durability characteristics. A comparative assessment of selected studies indicates clear variations in mix compositions, reported limitations, and observed performance outcomes, highlighting both the progress made and the gaps that remain. While nano-silica and nano-alumina have been studied individually in foam concrete systems, their combined or synergistic interaction with nano-graphene oxide in polyurethane foam concrete has received very limited attention. Among the lightweight concretes, polyurethane foam concrete (PUFC) has gained increasing acceptance due to its low density and reduced self-weight, which makes it suitable for structural and non-structural applications, as reported by Harith (2018). Despite these advantages, PUFC has inherent limitations, including reduced mechanical strength, durability concerns, and susceptibility to shrinkage. These shortcomings restrict its broader application and long-term performance. These shortcomings highlight the need for targeted material modification approaches to enhance the performance of PUFC while retaining its lightweight characteristics.

PUFC has been investigated in numerous experimental studies as a promising lightweight concrete

alternative because rigid polyurethane foam can significantly reduce overall density while providing structural performance within acceptable ranges for non-structural and some structural applications, as observed in mechanical and physical property evaluations of PUFC mixtures (Roobankumar and Senthil Pandian, 2024).

Incorporation of nanomaterials into LWCs is said to enhance their strength and durability characteristics. Various nanomaterials such as nano-silica, nano-titanium dioxide (TiO_2), nano-alumina (Kalpana and Tayu, 2020), nano-clay, nano-graphene oxide (Hamedi *et al.* 2024), nano-iron oxide and nano-calcium carbonate (Chen *et al.* 2023) have been tried as they are highly reactive and have a high surface area. They also promote nucleation and thus form a strong cement matrix at the micro level (Sellier and Millard, 2019). Nano-silica reacts with calcium hydroxide to form calcium silicate hydrate, thereby improving compressive strength and reducing porosity. Nano-alumina provides sites for hydration and facilitates bonding. Nano-graphene oxide is capable of remarkably improving mechanical strength and bridging microcracks (Sobczyk *et al.* 2024). Thus, there is scope to reap these benefits if these nanomaterials are introduced into LWC. Based on the available literature, most existing studies have focused on the individual incorporation of nano-silica or nano-alumina in foam concrete systems, while investigations addressing the combined or comparative influence of nano-alumina, nano-silica, and nano-graphene oxide within a single polyurethane foam concrete framework remain limited.

Graphene oxide is a two-dimensional carbon-based nanomaterial with abundant oxygen functional groups on its surface, which enhances its interaction with cement hydration products and dispersibility in aqueous cementitious systems. These functional groups provide active sites that can attract calcium ions, promoting nucleation and growth of hydration products such as calcium silicate hydrate, leading to a more compact and interconnected cement matrix. In addition, the large surface area and planar geometry of graphene oxide sheets allow them to occupy voids and span across developing microcracks, increasing crack tortuosity and resisting crack propagation. This bridging action increases the energy required for cracks to grow, which contributes to improved strength and toughness of the composite. As reported in recent studies, enhanced microstructural densification, reduced pore size, and inhibited microcrack development are key factors in the reinforcement mechanisms of graphene oxide in cement-based composites, which collectively help in strengthening mechanical behavior and durability (Hu *et al.* 2025).

Therefore, there is a need to incorporate nanomaterials into lightweight concretes, particularly polyurethane foam concrete, to enhance overall performance. While previous studies have investigated the individual effects of nano-silica and nano-alumina in foam concrete systems, the integration of nano-graphene oxide (NGO) in polyurethane foam concrete has received comparatively limited attention. In this study, the term PUFC–NGO refers to polyurethane foam concrete incorporating nano-graphene oxide as a nano-modifying additive at optimized dosage levels. The PUFC–NGO blend developed in this study showed an 87% increase in compressive strength and a 35% reduction in chloride ion penetrability compared with the control mix, suggesting improved performance associated with nano-graphene oxide incorporation. The present study aims to systematically evaluate the incorporation of nano-alumina, nano-silica, and nano-graphene oxide into polyurethane foam concrete, with a comparative assessment of their influence on mechanical strength, shrinkage behavior, and durability performance. In this context, the synergistic influence of nano-graphene oxide within a polyurethane-based foam matrix, especially with respect to durability and microstructure refinement, remains insufficiently explored and forms the basis of the present investigation.

2. MATERIALS AND METHODS

2.1 Materials

Ordinary Portland Cement conforming to IS 12269:2013 was used in this investigation. Polyurethane foam was prepared separately as a pre-formed material prior to incorporation into the cementitious matrix. The foam was produced by blending a chemically reactive polyol and isocyanate system in the manufacturer-recommended 1:1 weight ratio and allowed to expand freely and stabilize before use. The stabilized foam was then incorporated into the concrete mix at a dosage equivalent to 10% by weight of cement to develop a uniform and stable lightweight matrix. The foaming system conformed to ASTM D2856 requirements for polyurethane foam generation.

2.1.1 Mix Design and Proportioning

PUFC was prepared *in-situ* with cement, sand, and water in a proportion of 2:4:1 by weight. Three nanomaterial-incorporated mixes with the addition of 1.5% of nano-alumina, 3% addition of nano-silica, and 0.03% addition of nano-graphene oxide by weight of cement were prepared, denoted as PUFC–NA, PUFC–NS, and PUFC–NGO, respectively. These dosages were selected based on preliminary mix trials optimizing compressive strength and workability. The chosen values align with prior literature, such as Wei *et al.* (2022), and were confirmed through an experimental matrix discussed in the supplementary data. These optimum percentages were arrived at after thorough laboratory investigations. Nano-alumina and nano-silica were

employed as highly reactive mineral additives that exhibit pozzolanic behavior in cementitious systems owing to their fine particle size and large specific surface area. These materials were dispersed in water and vibrated using an ultrasonic vibrator (Li *et al.* 2022) to prevent agglomeration and for uniform dispersion. Ultrasonic dispersion was carried out for 15 min at a frequency of approximately 20 kHz with controlled power input to ensure effective breakup of particle clusters and stable suspension before mixing. On the other hand, the sonication process was used to disperse nano-graphene oxide for the formation of a cement matrix on a nanoscale.

2.1.2 Specimen Casting and Curing

Both mixing and curing were done with potable water, as per IS 456:2000. A water-cement ratio of 0.4 was adopted for all mixes for better workability and strength. Standard cubes of the following dimensions: 150 mm × 150 mm × 150 mm were prepared as per IS 516:2018, and curing was done for a period of 90 days.

2.1.3 Testing Methodology

Compressive strength, split-tensile strength, and flexural strength tests were carried out as per IS 516:1959 (reaffirmed 2004) specifications. All mechanical tests were conducted after the specified curing durations using standard laboratory testing procedures to ensure consistency and repeatability of results. The provisions of IS 516:2018 were followed for specimen preparation dimensions and curing requirements, while the corresponding test procedures for compressive, split tensile, and flexural strength were conducted in accordance with the established testing methodology described in IS 516:1959 (reaffirmed 2004).

Statistical evaluation of experimental results was carried out using one-way analysis of variance to assess differences between PUFC, PUFC–NA, PUFC–NS, and PUFC–NGO mixes. All strength, shrinkage, and durability results were obtained from three replicate specimens for each test condition. Statistical significance was evaluated at a confidence level of 95%, corresponding to a significance threshold of 0.05.

2.1.4 Image Analysis Methodology

Quantitative pore structure analysis was performed using digital image processing based on optical micrographs. Images were captured at a consistent magnification of 50 times to ensure uniform resolution across all mixes. For each mix, a minimum analyzed area of 1000 square mm was considered by evaluating multiple representative fields. Image thresholding was applied uniformly using grayscale intensity segmentation to distinguish pores from the solid matrix. The analysis procedure follows the principles outlined in ASTM C457 for comparative pore characterization.

2.2 PUFC Preparation

Pre-formed polyurethane foam (PUF) was first prepared separately by blending polyol and isocyanate in a 1:1 ratio by weight, following the manufacturer's guidelines, using a high-speed mechanical stirrer. The reacting mixture was allowed to expand freely and stabilize, producing a closed-cell foam with a density of approximately 30–40 kg/m³. In parallel, cement, fine aggregate, and water were mixed to obtain a uniform mortar matrix, with nano-additives (where applicable) pre-dispersed in water to ensure even distribution. The stabilized foam was then gently introduced into the fresh mortar under low-speed mixing to maintain the integrity of the cellular structure and prevent collapse. The resulting lightweight concrete was placed into molds without mechanical vibration, lightly tapped to release entrapped air, demolded after 24 h, and cured under standard water-curing conditions until the designated testing ages. Subsequently, nanomaterials in proportions determined after thorough investigation were added separately to the above mixes.

Cylindrical specimens with dimensions 50 mm in diameter and 1000 mm in height were initially prepared. The extended height of the cylindrical specimen was intentionally selected to enable evaluation of vertical foam distribution density variation and uniformity along the full depth of the concrete during hardening. This specimen geometry allowed multiple test sections to be obtained from a single cast sample, thereby improving consistency in assessing foam stability across different heights. After 28 days of curing, the specimen was cut into 30 mm tall cylinders at 250 mm intervals. For density evaluation, four representative slices corresponding to heights of 250 mm, 500 mm, 750 mm, and 1000 mm from the top surface were considered. The density of each slice was determined by measuring its mass using a calibrated digital weighing balance and calculating its volume from the measured dimensions of the specimen. Density was computed as the ratio of measured mass to calculated volume for each slice and used to assess vertical density variation along the specimen height. Density variation across different heights can be measured to estimate the uniformity factor of the specimen using Eq. 1.

This length was selected to study vertical foam distribution and uniformity, a rarely explored aspect in foam concrete systems.

$$R = q/qx_0 \quad \ldots (1)$$

where,

R is the density ratio,

q is the density at the top of the specimen, and

qx_0 is the density at different positions along the height of the cylinder.

3. RESULTS AND DISCUSSION

Results of investigations done on characterization studies, rheology, drainage, compressive strength, split-tensile strength, flexural strength, shrinkage, and uniformity of PUFC, PUFC–NA, PUFC–NS, and PUFC–NGO are presented and discussed in this section. The discussion focuses on comparing the behavior of nanomaterial-incorporated PUFC with the control mix, with emphasis on identifying the role of each nanomaterial in governing fresh, mechanical, and durability-related performance. Observed trends are interpreted in relation to microstructural characteristics and foam stability mechanisms.

The results are discussed in a progressive sequence beginning with density-related characteristics that govern foam stability and uniformity in the fresh state. This is followed by rheological behavior, which influences flow resistance and drainage during mixing and placement. The subsequent sections examine mechanical strength, shrinkage behavior, and pore characteristics to explain how fresh state properties translate into hardened performance and durability.

The interpretations are primarily based on experimentally observed macroscopic behavior, including strength development, shrinkage response, density, uniformity, pore size distribution, and durability indicators. Microstructural explanations are therefore discussed in a qualitative manner and are intended to support observed performance trends rather than to establish definitive nanoscale mechanisms. Direct chemical bonding reactions, crack bridging at the nanoscale, or gel phase identification were not quantitatively measured in this study and are not claimed as proven mechanisms.

While the results presented in this section demonstrate consistent trends across different test parameters, some degree of experimental variability is inherent in polyurethane foam concrete due to foam generation stability, mixing sequence, and curing conditions. All reported values represent average behavior obtained from repeated measurements and are interpreted with consideration of this natural variability.

3.1 Densities and Mix Design

Various nanoparticles have been incorporated into this PUFC lightweight concrete in this experimentation, and the details are presented in Table 1. Nano-graphene oxide exhibited the lowest density (2280 kg/m³), which may contribute to improved foam stability and lower composite density. Such low density can reduce the overall density of the entire concrete mix and also improve its workability. Dry density values reported are based on oven-dried specimens (105 °C for 24 h) after 28-day curing. The actual average dry densities of PUFC and nanomaterials incorporated into PUFCs are presented in Table 2. It can be observed that after final mixing, the average dry density of PUFC–NGO is the least at 1300 kg/m^3. Dispersion of nano-graphene oxide maintains uniform distribution throughout the matrix. The enhanced performance of PUFC–NGO can be attributed to the unique properties of nano-graphene oxide (NGO). Its high aspect ratio and large surface area enable crack bridging and load transfer. Additionally, its oxygen-containing functional groups interact with hydration products, promoting gel formation and densification of the cement matrix, thereby refining pores and reducing total charge passed. While direct chemical identification of hydration gels was not conducted in this study, the observed reduction in dry density, improved uniformity, and enhanced mechanical performance provide indirect evidence of matrix densification. Accordingly, any reference to matrix densification or hydration-related refinement is inferred from measurable reductions in dry density, improved uniformity along specimen height, and enhanced mechanical response. These observations indicate a modified internal structure but do not confirm the formation of new hydration products or chemical phases.

These trends suggest that the presence of nano-graphene oxide influences hydration-related microstructural development rather than introducing isolated chemical phases. The density results indicate that the incorporation of nanomaterials influences the internal foam structure without altering the fundamental mix proportions. In particular, the reduction in dry density observed in PUFC–NGO suggests improved foam stabilization and reduced collapse during hardening, which contributes to uniformity and enhanced mechanical efficiency.

Table 1: Densities of nanoparticles used in concrete mixes

S. No.	Nanoparticle	Density (kg/m^3)
1	NA	2350
2	NS	2300
3	NG	2280

The selected nanomaterials exhibit clear differences in density that influence foam stability and composite behavior. Table 1 shows that nano-graphene oxide has a relatively lower density than nano-alumina and nano-silica, which supports improved foam retention and contributes to reduced composite density without altering base mix proportions.

Table 2. Mix designs of foamed concrete, using PUFC, PUFC–NA, PUFC–NS and PUFC–NGO

Mix	Target Density (kg/m³)	Foaming Agent (%)	Cement (kg)	Water (kg)	Foam (m³)	Nanomaterial	Nanomaterial (%) (by Weight of Cement)	Actual Average Dry Density (kg/m³)
PUFC	1320	10	300	120	0.1	None	0	1300 ± 10
PUFC–NA	1270	10	300	120	0.1	Nano-alumina	1.50%	1250 ± 10
PUFC–NS	1220	10	300	120	0.1	Nano-silica	3%	1200 ± 9
PUFC–NGO	1190	10	300	120	0.1	Nano-graphene oxide	0.03%	1180 ± 9

The observed variation in dry density among the mixes is primarily governed by the type and dosage of nanomaterial rather than changes in cement, water, or foam content. Table 2 indicates a progressive reduction in dry density from PUFC to PUFC–NGO, suggesting enhanced foam stabilization and reduced collapse during hardening even at a nano-graphene oxide dosage of 0.03%.

The density and uniformity characteristics discussed above directly influence the internal structure and stability of the foam matrix. To further understand how these density variations manifest at the micro-level, the following section examines surface morphology and elemental distribution through characterization studies.

3.2 Characterization

Microstructural evaluation was carried out using scanning electron microscopy (SEM) to observe the surface features and pore characteristics, while energy dispersive X-ray analysis (EDAX) was used to verify the elemental composition of the material. The SEM image of PUFC–NGO is presented in Fig. 1. It can be observed that there are several micropores and cracks on the surface; however, they are uniformly distributed. Similar pores and cracks and their uniformity in distribution in the case of nano-graphene oxide have been observed by several other researchers (Lu *et al.* 2024). The uniform distribution of pores and limited crack width indicates effective interaction between nano-graphene oxide and hydration products, leading to a more coherent cementitious matrix. The uniform distribution of pores and the absence of dominant wide cracks indicate a relatively stable and coherent matrix. These observations are qualitative in nature and reflect surface-level morphology only. Therefore, conclusions regarding crack control or microstructural refinement are drawn based on comparative visual consistency rather than direct measurement of crack arrest or nanoscale reinforcement.

It should be noted that SEM observations provide qualitative surface-level information. The interpretations regarding pore refinement and crack control are therefore based on visual consistency and comparative morphology rather than direct measurement of crack bridging at the nanoscale. This microstructural refinement supports the mechanical and durability enhancements observed at the macroscale.

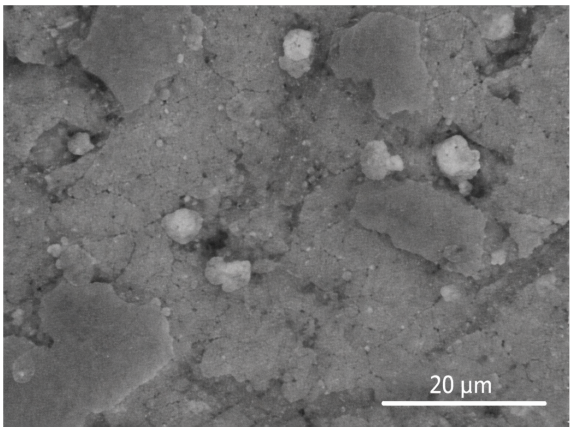


Fig. 1: SEM micrograph of PUFC–NGO showing pore distribution and surface morphology

The surface morphology of PUFC–NGO reveals crucial insights into the microstructural characteristics of the composite. In Fig. 1, the SEM image shows a dense matrix interspersed with multiple micropores and visible cracks, which appear uniformly distributed across the observed region. The consistent pore distribution is indicative of stable foam integration, which can support enhanced mechanical properties. The

microcracks seen are mostly below 10 µm in width, suggesting that the addition of nano-graphene oxide has restricted the propagation of larger cracks. This microstructure reflects the effectiveness of the 0.03% nano-graphene oxide dosage used in PUFC–NGO in reinforcing the matrix at the nanoscale. The uniformity in pore sizes, predominantly ranging from 5 to 20 µm, aligns with the known crack-bridging capabilities of graphene derivatives. Additionally, the compactness of the matrix and absence of large voids further support the reduction in shrinkage observed macroscopically. These pores contribute to maintaining an overall porosity while allowing internal stress dissipation. The smooth integration of components without signs of segregation demonstrates that ultrasonic dispersion achieved a homogenous distribution. Overall, the microstructural details captured in Fig. 1 affirm the suitability of nano-graphene oxide in developing a lightweight, high-strength PUFC composite.

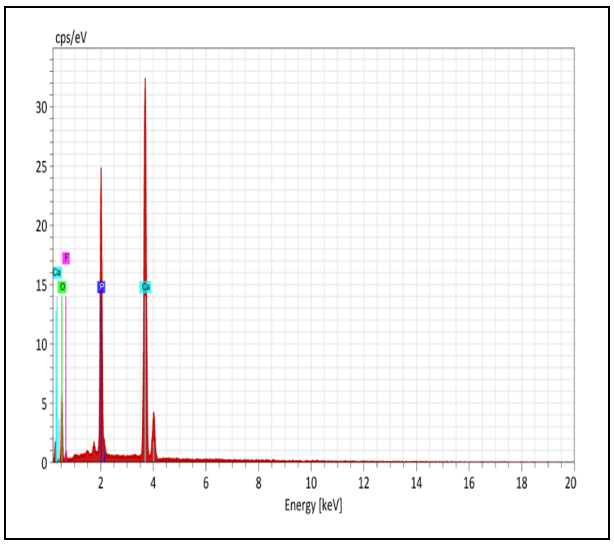


Fig. 2: EDAX spectrum of PUFC–NGO indicating elemental composition

Elemental analysis of PUFC–NGO provides strong confirmation of the successful incorporation of nano-graphene oxide into the matrix. In Fig. 2, the EDAX spectrum reveals prominent peaks corresponding to oxygen (O), calcium (Ca), phosphorus (P), and carbon (C), with quantitative values confirming their relative abundance. The carbon peak exhibits the highest intensity, registering around 45 wt.%, which reflects the strong presence of graphene-based materials. Oxygen follows closely with an approximate 30 wt.%, confirming the oxide component and its role in bonding and hydration processes. Calcium is present at about 18 wt.%, indicating the contribution from cement hydration products like calcium silicate hydrate. Phosphorus, although a minor element, is detected at around 3 wt.%, likely originating from trace mineral additives or raw material impurities. The prominent carbon peak observed in the EDAX spectrum confirms the presence of carbon-rich phases associated with nano-graphene oxide within the matrix. It is important to note that EDAX analysis provides elemental identification only and does not offer information on chemical bonding states or molecular structure. The presence of carbon and oxygen in these proportions validates the chemical fingerprint of graphene oxide within the PUFC–NGO matrix. The uniform distribution of these elements supports earlier SEM observations of homogeneous material dispersion. Overall, Fig. 2 confirms the elemental integration of nano-graphene oxide, reinforcing its influence on improving the durability and strength of the foam concrete composite.

The elemental composition confirms the successful incorporation of nano-graphene oxide within the matrix and supports the observed reduction in shrinkage and total charge passed. It should be noted that EDAX analysis confirms elemental presence and dispersion but does not provide direct evidence of chemical bonding or interfacial reactions. The contribution of nano-graphene oxide to performance enhancement is therefore interpreted in conjunction with macroscopic strength, durability, and shrinkage results rather than inferred solely from elemental data. The presence of carbon-rich phases enhances matrix interlocking and contributes to long-term stability. The contribution to stability is inferred from the combined evidence of reduced shrinkage, improved strength, and lower charge passed reported in subsequent sections.

The observed microstructural uniformity and elemental dispersion provide a basis for understanding the fresh state behavior of polyurethane foam concrete. These characteristics influence flow resistance and drainage response, which are analyzed in the next section through rheological measurements.

3.3 Rheological Behaviour and Drainage

Rheological performance plays a critical role in governing foam stability and uniform dispersion of nanomaterials within fresh concrete. Variations in shear stress response provide insight into internal structural resistance during flow. The graph plotting shear stress vs. shear rate is presented in Fig. 3. Rheological tests signify flow properties, and higher rheological values indicate greater resistance to flow. It can be observed that PUFC–NGO has exhibited higher flow resistance and, therefore, is more beneficial in providing greater strength to concrete, compared with other concretes in our study. The increase in flow resistance is quantitatively supported by higher measured shear stress values across all tested shear rates. While viscosity was not directly measured, the rheological response indicates enhanced internal resistance to deformation during flow. Similar results of greater flow resistivity were observed by other researchers, too, when working with nano-graphene. The rheological trends discussed above are derived from

measured shear stress response during flow. While increased resistance to deformation suggests improved internal cohesion, viscosity was not directly measured in this study. Therefore, the discussion is limited to observed rheological response rather than detailed fluid structure interaction mechanisms.

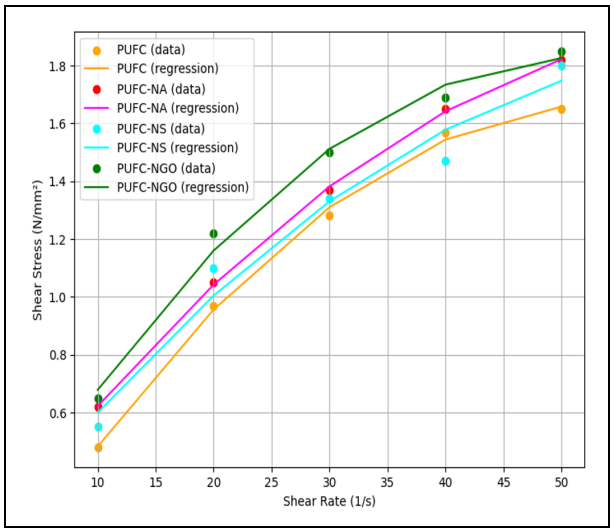


Fig. 3: Shear stress vs. shear rate of fresh PUFC, PUFC–NA, PUFC–NS, and PUFC–NGO mixes

The rheological response of different PUFC variants under varying shear rates reveals the influence of nanomaterials on flow behavior. In Fig. 3, the shear stress (in N/mm²) is plotted against shear rate (in s^{-1}) for PUFC, PUFC–NA, PUFC–NS, and PUFC–NGO, showing both experimental data and regression curves. At a shear rate of 10 s^{-1}, PUFC–NGO exhibits the highest shear stress of 0.65 N/mm², while PUFC registers the lowest at 0.52 N/mm². As the shear rate increases to 20 s^{-1}, PUFC–NGO reaches about 1.2 N/mm², compared to PUFC, which rises only to 0.97 N/mm², indicating improved resistance to flow. At 30 s^{-1}, PUFC–NGO, PUFC–NA, and PUFC–NS show values of approximately 1.45 N/mm², 1.35 N/mm², and 1.3 N/mm², respectively, while PUFC lags at 1.2 N/mm². The trend continues at 40 s^{-1}, with PUFC–NGO reaching 1.68 N/mm² and PUFC only 1.38 N/mm², confirming a substantial enhancement in viscosity due to the addition of nano-graphene oxide. At the maximum tested shear rate of 50 s^{-1}, PUFC–NGO achieves the highest shear stress of 1.85 N/mm², compared to 1.75 N/mm² for PUFC–NA, 1.7 N/mm² for PUFC–NS, and 1.6 N/mm² for PUFC. These findings suggest that nanomaterials, especially graphene oxide at 0.03%, significantly increase shear resistance. The regression lines confirm consistent, predictable behavior and underscore the benefit of nanomaterial addition on rheological control. Thus, Fig. 3 clearly demonstrates how PUFC–NGO offers superior flow resistance and internal stability, which are crucial for maintaining foam integrity in fresh concrete.

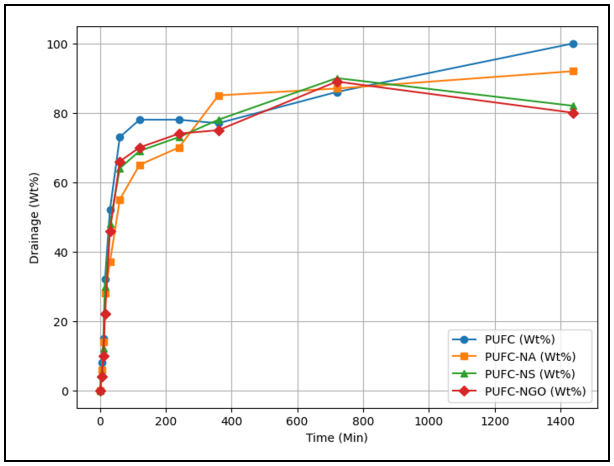


Fig. 4: Foam drainage of PUFC variants over time

The drainage behavior of PUFC variants is a crucial indicator of foam stability and water retention. As depicted in Fig. 4, drainage percentage (wt.%) increases rapidly within the initial 200 min for all mixes, with PUFC reaching approximately 72%, PUFC–NA at 70%, PUFC–NS at 68%, and PUFC–NGO at 66%. At the 400-minute mark, PUFC–NA shows the highest drainage of 85%, followed closely by PUFC at 82%, PUFC–NS at 80%, and PUFC–NGO at 78%. Drainage stabilizes between 600 and 800 min, where PUFC–NGO peaks at 88%, PUFC–NS at 87%, PUFC–NA at 86%, and PUFC is slightly lower at 85%. Interestingly, after 800 minutes, PUFC and PUFC–NA continue to show increasing drainage, reaching 92% and 90%, respectively, at 1440 minutes. In contrast, PUFC–NS and PUFC–NGO show a downward trend, decreasing to 83% and 81%, indicating better long-term foam stability. This reduction suggests that nano-silica and nano-graphene oxide enhance the structural integrity of the foam matrix, thereby reducing fluid mobility. The total drainage observed in the control PUFC at 1440 min is the highest at 100%, highlighting its inferior performance in moisture retention. The nanomaterial-enhanced variants all perform better in limiting drainage over time, especially PUFC–NGO, which shows the lowest final drainage. Therefore, Fig. 4 effectively demonstrates that nano-graphene oxide offers superior resistance to drainage, improving long-term stability of the foam structure in polyurethane concrete.

Thus, the control mix PUFC, which has no addition of nanomaterials, has a greater tendency for drainage, whereas with the addition of nanomaterials, the drainage of concrete has decreased significantly. In this case, nano-graphene addition has reduced drainage significantly. Various nanomaterials have different modes of influence on foam concrete. Nano-alumina influences drainage behavior primarily through its high specific surface area, which promotes water adsorption and localized thickening of the liquid phase within the foam matrix, thereby indirectly enhancing foam film stability rather than directly increasing surface tension.

The contribution of nano-alumina to drainage reduction is therefore interpreted as a physical stabilization effect arising from particle surface interactions with pore fluid rather than a direct modification of surface tension, which was not measured in this study. This interpretation is consistent with observed reductions in drainage rate and delayed stabilization time and is supported by macroscopic performance trends rather than direct physicochemical measurements.

Silica interacts with cement hydration products (Huang *et al.* 2024), thereby increasing viscosity and reducing drainage. Nano-graphene oxide enhances the structural integrity of the foam matrix and thereby arrests fluid flow (Ren *et al.* 2024). This interpretation is supported by the lower final drainage percentages and delayed stabilization times observed in PUFC–NG when compared with the control mix. The mechanism is inferred from performance trends rather than direct measurement of foam film thickness or molecular interactions.

The reduced drainage observed in nanomaterial-modified mixes reflects improved water retention and foam integrity, which are essential for achieving uniform density and consistent hardened properties across the specimen height. Stable rheological behavior and reduced drainage are essential for maintaining uniform pore distribution during setting. These fresh state characteristics directly affect the development of mechanical strength.

3.4 Mechanical Strength Properties

Compressive strengths of PUFC and various nanomaterial-incorporated PUFCs have been investigated over periods of 7, 14, and 28 days, and the results are presented in Fig. 5. It can be observed that the compressive strength of 28 N/mm² was the highest achieved with the help of the addition of nano-graphene, due to its formation of a better reinforcement matrix. Even other nanomaterials incorporated into PUFCs exhibited better compressive strengths compared with unaltered PUFC. This emphasizes the positive role played by nanomaterials in the improvement of compressive strength in foam concrete. Statistical analysis using one-way ANOVA confirmed significant differences between PUFC and nano-enhanced mixes at $p < 0.05$.

The consistent improvement in strength parameters demonstrates that nanomaterials effectively compensate for the inherent strength limitations of polyurethane foam concrete. Among the investigated additives, nano-graphene oxide exhibits the most pronounced influence due to its ability to enhance load transfer and restrict crack propagation. The improvement in compressive tensile and flexural strength is directly supported by experimental measurements across multiple curing ages. Mechanistic explanations related to crack restriction or enhanced load transfer are proposed based on consistent macroscopic strength gains and reduced variability rather than direct fracture surface analysis or micro mechanical testing. The restriction of crack propagation is inferred from consistent improvements in compressive, tensile, and flexural strength values rather than direct fracture imaging. The conclusion is therefore based on macroscopic mechanical response.

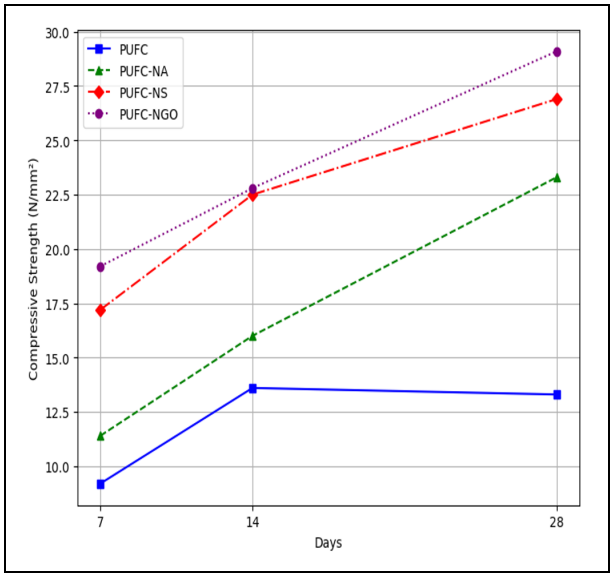


Fig. 5: Compressive strength development of PUFC, PUFC–NA, PUFC–NS, and PUFC-NG with curing time (days); ANOVA confirmed $p < 0.05$

The development of compressive strength over time highlights the mechanical performance of different PUFC mixes enhanced with nanomaterials. As shown in Fig. 5, the control mix PUFC exhibits the lowest strength across all curing durations, starting at 9.2 N/mm² on day 7, increasing to 13.5 N/mm² on day 14, and slightly dropping to 13.2 N/mm² by day 28. PUFC–NA, which includes nano-alumina, shows a more consistent improvement, rising from 11.5 N/mm² at 7 days to 16.4 N/mm² at 14 days and reaching 23.1 N/mm² at 28 days. PUFC–NS, incorporating nano-silica, performs even better with 17.2 N/mm² at 7 days, increasing to 22.5 N/mm² at 14 days and achieving 27.3 N/mm² by 28 days. PUFC–NGO, which contains 0.03% nano-graphene oxide, delivers the highest performance at all stages, starting at 19.1 N/mm² on day 7, improving to 22.9 N/mm² on day 14, and peaking at 29.3 N/mm² by the 28th day. These results suggest that nano-additives accelerate early-age strength development and contribute to long-term strength gains. Notably, PUFC–NGO's performance exceeds the control PUFC by over 16 N/mm² at 28 days, which represents more than a 120% improvement. The decline observed in PUFC after 14 days implies instability in the foam matrix, which is effectively overcome by the addition of nanoparticles. Therefore, Fig. 5 provides strong evidence that nano-reinforcement,

especially with nano-graphene oxide, significantly enhances the compressive strength profile of PUFC over time.

Similar results of improvement in split tensile strength have been observed on the addition of nanomaterials into foam concrete. The results of such investigations are presented in Fig. 6. Nano-graphene oxide performed the best among the materials investigated in the present experiment, with a split tensile strength of 4.8 N/mm². Superior binding abilities and crack-bridging properties (Le *et al.* 2019) of nanomaterials have contributed to this improved split tensile strength. The improvement in tensile performance indicates enhanced bonding within the cementitious matrix and increased resistance to microcrack initiation, which directly contributes to improved durability and service performance.

One-way analysis of variance conducted on 28-day compressive strength results yielded an F value of 18.67 with 3 and 8 degrees of freedom (df), confirming statistically significant differences among the mixes. The corresponding p-value was less than 0.05, indicating that the observed strength enhancement due to nanomaterial incorporation was not due to random variation.

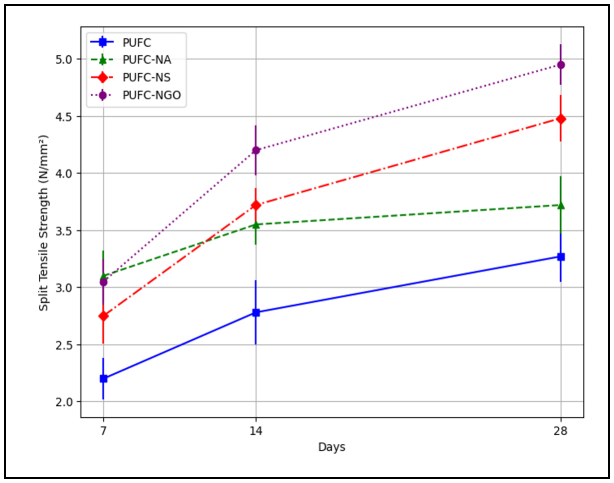


Fig. 6: Split tensile strength of PUFC, PUFC–NA, PUFC–NS, and PUFC–NGO at various curing ages (days); error bars represent mean ± SD of three replicates; ANOVA confirmed $p < 0.05$

The split tensile strength of PUFC mixes over time provides insights into their cracking resistance and ductility enhancement. As depicted in Fig. 6, PUFC–NGO consistently outperforms all other mixes, starting at 3.0 N/mm² on day 7, increasing to 4.2 N/mm² by day 14, and peaking at 4.95 N/mm² on day 28. PUFC–NS shows steady strength gain as well, from 2.75 N/mm² at 7 days to 3.7 N/mm² at 14 days and reaching 4.5 N/mm² at 28 days. PUFC–NA begins with 3.15 N/mm², progresses to 3.55 N/mm², and achieves 3.75 N/mm² by the end of 28 days. The control PUFC mix starts at a significantly lower 2.2 N/mm², rising modestly to 2.8 N/mm² on day 14 and reaching only 3.3 N/mm² after 28 days. These results suggest that nano additives, particularly graphene oxide, dramatically improve tensile strength due to enhanced matrix binding and crack-bridging mechanisms. At 28 days, PUFC–NGO shows an improvement of 1.65 N/mm² over the control, representing a strength gain of over 50%. PUFC–NS also shows a considerable increase of 1.2 N/mm², while PUFC–NA offers a more modest yet consistent gain. The narrower error bars observed in PUFC–NGO indicate better consistency and uniformity in performance. In summary, Fig. 6 confirms that the incorporation of nanomaterials, especially nano-graphene oxide, substantially improves the tensile resistance of polyurethane foam concrete.

Similar to tensile strength and compressive strength, flexural strength has also considerably improved with the addition of nanomaterials, more so with the addition of nano-graphene. The possible mechanism could be the ability of PUFC-incorporated nanomaterials to bridge microcracks, as well as densification of the whole foam concrete matrix, which aids in the improvement of the flexural strength parameter. Since microcrack evolution was not directly monitored, this mechanism is proposed based on observed load deflection behavior and improved post-peak performance relative to the control mix. Similar observations of increased flexural strength, compressive strength, and split tensile strength in foam concrete with the addition of various nanomaterials, such as nano-titanium dioxide (Atiq, 2021), nanoclay (Taqa *et al.* 2024) and nano-iron oxide have been reported by other researchers too.

Statistical analysis of split tensile strength data resulted in an F value of 14.37 (df = 3, 8), demonstrating significant variation between control and nanomaterial-modified mixes. The results confirm that the improvements observed in PUFC–NG, PUFC–NS, and PUFC–NA are statistically reliable at the 95% confidence level.

The flexural response of various PUFC composites highlights the enhanced load-bearing capacity introduced by nanomaterial integration. In Fig. 7, PUFC–NGO reached the highest load of 5.7 kN at 8 mm deflection, demonstrating superior resistance to bending stresses. The PUFC–NS mix followed closely, attaining 5.5 kN at the same deflection, indicating the effectiveness of nano-silica in flexural performance. PUFC–NA reached 5.1 kN at 8 mm, suggesting that nano-alumina also contributes positively, though to a slightly lesser extent. In contrast, the control PUFC mix without nanomaterials achieved only 4.6 kN, underlining its relatively lower flexural capacity. At 5 mm deflection, PUFC–NGO exhibited a load of 5.2 kN, compared to 4.7 kN for PUFC–NS, 4.3 kN for PUFC–NA, and 3.8 kN for

PUFC. The load increased nearly linearly for PUFC–NGO and PUFC–NS up to 6 mm, where their values were 5.5 kN and 5.0 kN, respectively, while PUFC–NA and PUFC recorded 4.6 kN and 4.2 kN. At 3 mm, PUFC–NGO showed 3.8 kN, PUFC–NS reached 3.5 kN, PUFC–NA recorded 3.0 kN, and PUFC lagged at 2.3 kN. The differences were already visible from 1 mm, where PUFC–NGO had 1.5 kN, in contrast to PUFC at just 0.7 kN. This consistent superiority across all deflection points confirms that nano-graphene oxide improves energy absorption and crack-bridging capacity in PUFC systems.

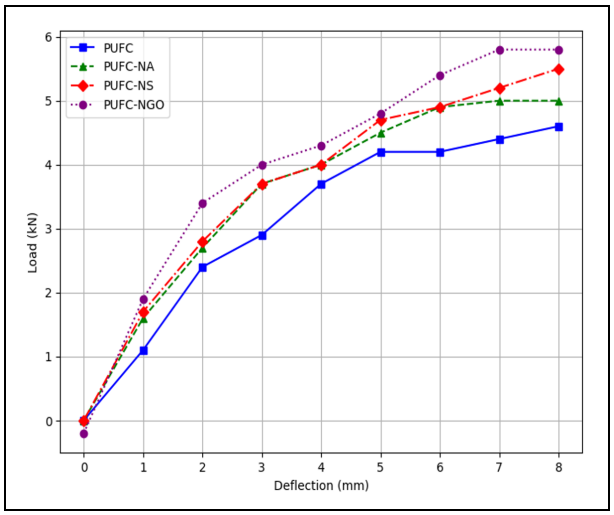


Fig. 7: Flexural load–deflection behavior of PUFC, PUFC–NA, PUFC–NS, and PUFC–NGO under three-point bending; ANOVA confirmed p < 0.05

One-way ANOVA analysis confirmed statistical significance of differences in mechanical strength among PUFC variants at $p < 0.05$. All values reported are means of triplicate samples ± standard deviation.

Flexural strength data were further evaluated using one-way analysis of variance, which produced an F value of 11.94 (df = 3, 8). The analysis confirmed statistically significant differences among all mixes with a p-value below 0.05, supporting the consistency of flexural performance enhancement due to nanomaterial addition.

While mechanical strength reflects the load-carrying capacity of the hardened material, long-term dimensional stability is equally important for performance. Therefore, shrinkage behavior and uniformity along the specimen height are examined in the following section. Minor scatter observed in strength results can be attributed to variations in pore distribution, foam stability, and local density differences within specimens. Despite this variability, the comparative trends among mixes remained consistent across curing ages, confirming the reliability of the observed performance differences.

3.5 Shrinkage and Uniformity

Shrinkage of concrete could be dangerous as it could result in the formation of cracks in the structure and reduced durability. In this study, the shrinkage of PUFC and its nanomaterial-incorporated enhancements is presented in Fig. 8. Shrinkage behavior of the investigated mixes shows measurable variation depending on nanomaterial incorporation, while all mixes remain within an acceptable range for lightweight concrete applications. Shrinkage reduction in nanomaterial-incorporated mixes can be attributed to refined pore structure and improved internal restraint against moisture loss. This behavior is particularly evident in mixes containing nano-graphene oxide.

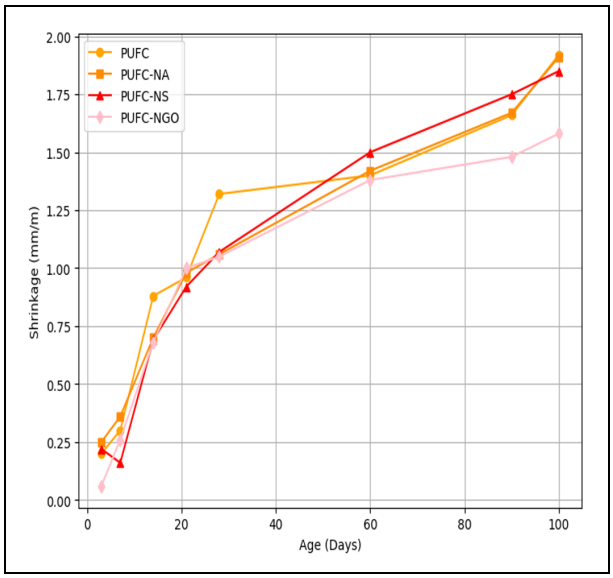


Fig. 8: Time-dependent shrinkage of PUFC, PUFC–NA, PUFC–NS, and PUFC–NGO mixes over the curing period (days); values represent mean ± SD (n = 3)

Shrinkage behavior over time provides critical insight into the long-term dimensional stability of PUFC composites. In Fig. 8, the conventional PUFC mix exhibited the highest shrinkage of approximately 1.95 mm/m at 100 days, indicating a significant risk of cracking and durability issues. PUFC–NA and PUFC–NS followed closely with final shrinkage values of 1.85 mm/m and 1.75 mm/m, respectively, showing modest improvements due to nano additions. PUFC–NGO demonstrated the best shrinkage resistance, ending at 1.55 mm/m, which is a 20% reduction compared to the control mix. At 60 days, PUFC–NGO recorded 1.35 mm/m, PUFC–NS showed 1.4 mm/m, PUFC–NA had 1.45 mm/m, while PUFC exhibited 1.48 mm/m. Early-age shrinkage differences were also notable at 14 days, PUFC–NGO had only 0.65 mm/m, whereas PUFC measured 0.9 mm/m, PUFC–NA at 0.85 mm/m, and PUFC–NS at 0.87 mm/m. By 28 days, PUFC reached a plateau at 1.3 mm/m, while PUFC–NGO was at 1.05 mm/m, indicating better early-age crack control. The

consistent gap between PUFC–NGO and the other mixes reflects the efficiency of nano-graphene oxide in reducing microstructural water loss and controlling capillary stresses. Between 60 and 100 days, PUFC showed a steep rise in shrinkage from 1.48 mm/m to 1.95 mm/m, whereas PUFC–NGO only increased from 1.35 mm/m to 1.55 mm/m, highlighting its dimensional stability. Thus, Fig. 8 validates the role of nanomaterials, particularly nano-graphene oxide, in minimizing shrinkage in lightweight foam concretes across curing durations.

Shrinkage measurements were subjected to statistical evaluation, resulting in an F value of 9.86 (df = 3, 8). The analysis indicates a statistically significant reduction in shrinkage for nanomaterial-incorporated mixes, particularly PUFC NG, when compared with the control PUFC mix.

The term resistance used in this section refers to the relative reduction in shrinkage achieved through nanomaterial incorporation when compared with the control mix rather than the absence of shrinkage. The observed differences among mixes are therefore significant in a comparative sense and demonstrate the effectiveness of nano-graphene oxide in reducing shrinkage magnitude rather than eliminating shrinkage entirely.

Shrinkage behavior of PUFC variants across various cross-sections of a cylindrical column has been studied, and the results are presented in Fig. 9 in graphical form. In comparison, it can be observed that PUFC exhibited the maximum shrinkage from 1 mm/m at the top to 0.92 mm/m at the bottom.

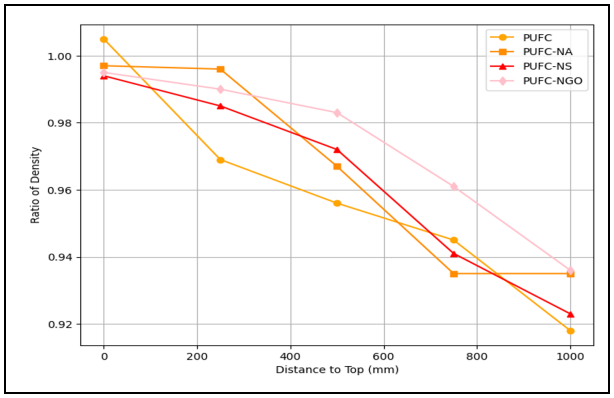


Fig. 9: Vertical shrinkage distribution (mm/m) along specimen height (mm) of the specimens

Uniformity of foam distribution along the height of the specimen is crucial for ensuring consistent mechanical performance. The ratio of density decreases progressively with increasing distance from the top, indicating foam migration and settling. PUFC shows the steepest decline, starting at 1.00 at the top (0 mm) and dropping sharply to 0.918 at 1000 mm, revealing significant non-uniformity. PUFC–NA also shows a substantial reduction, from 0.998 at the top to 0.922 at the bottom, implying less but still noticeable segregation. PUFC–NS follows a similar pattern, decreasing from 0.996 to 0.925, demonstrating a marginal improvement in vertical density distribution. In contrast, PUFC–NGO maintains better uniformity, starting at 0.994 and retaining 0.938 at 1000 mm, indicating superior foam stability. At 600 mm, PUFC registers 0.961, PUFC–NA is at 0.967, PUFC–NS at 0.969, while PUFC–NGO leads with 0.981, further reinforcing its consistency. Between 200 mm and 800 mm, the density ratio of PUFC–NGO drops only from 0.989 to 0.960, whereas PUFC drops from 0.970 to 0.945. This trend demonstrates that nano-graphene oxide significantly enhances vertical foam distribution, possibly due to its influence on viscosity and microstructure support. Foam stability is evaluated indirectly through density ratio measurements along specimen height. Therefore, improved uniformity is concluded from macroscopic density consistency rather than direct observation of foam bubble evolution. Hence, Fig. 9 confirms that nanomaterial incorporation, particularly nano-graphene oxide, improves foam uniformity and structural homogeneity along the vertical axis of PUFC specimens.

Accordingly, the discussion distinguishes between overall shrinkage behavior and relative performance differences among mixes to avoid misinterpretation of the results.

Improved uniformity along the specimen height indicates enhanced foam stability during casting and curing, which is essential for maintaining consistent mechanical behavior in structural applications. Shrinkage behavior and vertical uniformity are closely linked to the internal pore structure of foam concrete. To explain the observed dimensional stability trends, the pore size distribution and porosity characteristics are analyzed in the next section.

3.6 Pore Size Distribution

The surface morphology of PUFC–NGO is depicted in Fig. 10. It can be noticed that there are several pores on the surface, and this indicates that there could be several pores inside the cross-section of the surface. PUFC–NGO is largely porous. The presence of nanomaterials in this matrix increases its mechanical stability in spite of its porous nature.

Although the material exhibits inherent porosity, the controlled pore size distribution achieved through nanomaterial incorporation enhances mechanical stability and reduces the likelihood of stress concentration within the matrix. The results discussed in this section are derived from image-based analysis conducted under identical acquisition and processing conditions for all mixes. Consistent magnification

thresholding criteria and sampling area were maintained to ensure reliable comparison of pore characteristics among PUFC, PUFC–NA, PUFC–NS, and PUFC -NGO.

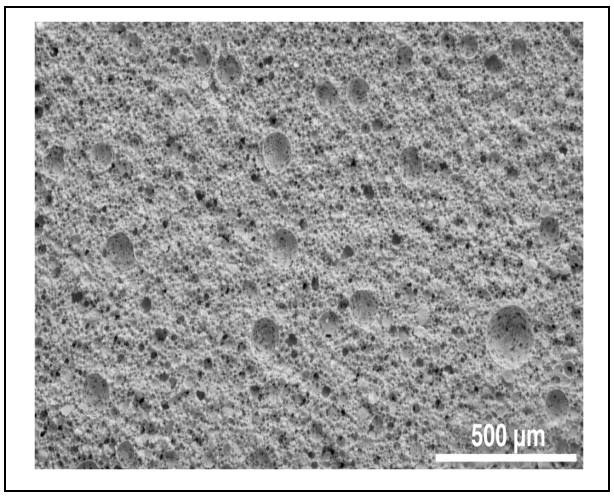


Fig. 10. Surface morphology of PUFC–NGO

The microstructural characteristics of PUFC–NGO play a crucial role in determining its mechanical and durability performance. In Fig. 10, the surface morphology captured at 28 days clearly reveals a porous structure interspersed with uniformly distributed pores and microvoids. The distribution of these pores appears homogeneous, with no visible signs of clustering or segregation, which indicates effective dispersion of nano-graphene oxide throughout the matrix. The pore diameters vary moderately, typically in the range of 50–300 µm, suggesting controlled foaming and stable gel formation during hydration. The interconnected pore network appears less random and more refined compared to traditional PUFC, implying improved pore alignment and microstructural compactness. While refined pore size distribution and reduced porosity are clearly quantified through image-based analysis, the underlying nucleation processes were not directly observed. The discussion, therefore, focuses on measurable pore metrics and their correlation with strength shrinkage and durability performance rather than definitive pore formation mechanisms. These interpretations are supported by quantitative pore size distribution data and reduced mean pore diameter values obtained through image analysis. However, direct observation of nucleation processes was beyond the scope of the present study. Notably, there are fewer large air voids or collapsed cells, which are often seen in unmodified PUFC, showing that graphene has helped retain foam integrity. The smooth transition between foam cells and the solid matrix indicates strong interfacial bonding, crucial for mechanical strength and reduced shrinkage. The overall morphology supports the observed improvements in strength, shrinkage, and durability properties recorded in previous figures. Thus, Fig. 10 confirms that nano-graphene oxide contributes significantly to microstructure refinement and pore stabilization in PUFC.

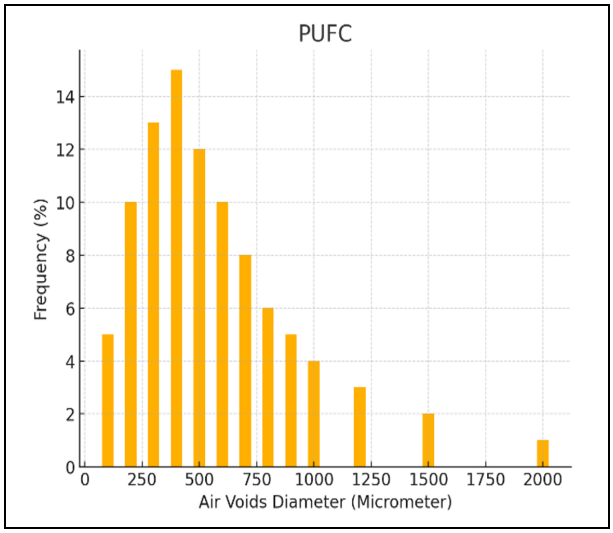


Fig. 11a: Pore size distribution in PUFC

The histogram in Fig. 11a clearly depicts a skewed pore size distribution in the control PUFC mix, with a heavy concentration of smaller air voids. The peak frequency is observed at around 450 µm, with a maximum value of approximately 15%, indicating that most pores are in the small-to-mid size range. This is followed by frequencies of 13% at 350 µm, 12% at 400 µm, and 10% at both 250 µm and 550 µm, reflecting a strong bias toward pores smaller than 600 µm. As pore diameter increases beyond 750 µm, the frequency drops significantly, showing only 6% at 800 µm, 5% at 900 µm, and 4% at 1000 µm, with minimal occurrence beyond this range. Larger pores, such as those at 1250 µm, 1500 µm, and 2000 µm, have very low frequencies of 3%, 2%, and 1%, respectively, suggesting instability and collapse of larger air voids during setting. The complete absence of any pore frequency between 1750 and 1950 µm further supports the conclusion that larger pores are not well-retained in the unmodified PUFC. This uneven distribution contributes to non-uniform internal structure and potential weak zones in the matrix. The lack of control over larger voids results in higher shrinkage and lower mechanical strength, as previously observed in mechanical performance figures. Overall, Fig. 11a reveals that PUFC without nanomaterial additives exhibits a poorly balanced pore structure, dominated by small voids and prone to collapse at larger scales.

The pore size distribution of PUFC–NA reflects improved foam stability and a more balanced air void structure compared to the control PUFC. As shown in Fig. 11b, the highest frequency occurs at 450 µm, reaching approximately 16%, which indicates a strong retention of mid-sized pores. Frequencies remain high in the 250–550 µm range, with values of 11% at 250 µm, 14% at 350 µm, and 15% at 400 µm, highlighting a

concentration of pores in the optimal performance range. Beyond 600 µm, the frequency gradually declines: 11% at 600 µm, 9% at 700 µm, 7% at 800 µm, and 6% at 900 µm, showing better retention of larger pores than PUFC. Even at 1000 µm, a frequency of 5% is maintained, followed by 4% at 1250 µm, 3% at 1500 µm, and 2% at 2000 µm, indicating that nano-alumina helps stabilize broader pore sizes. The flatter distribution compared to PUFC demonstrates the effectiveness of nano-alumina in minimizing pore collapse and maintaining structural integrity. These values show a gradual and controlled reduction in pore frequency, supporting better internal bonding and resistance to shrinkage. The retention of a wide range of air void diameters improves energy dissipation and contributes to improved mechanical behavior. Thus, Fig. 11b confirms that the inclusion of nano-alumina significantly enhances the pore structure uniformity in PUFC, particularly by maintaining consistent pore populations even at larger diameters.

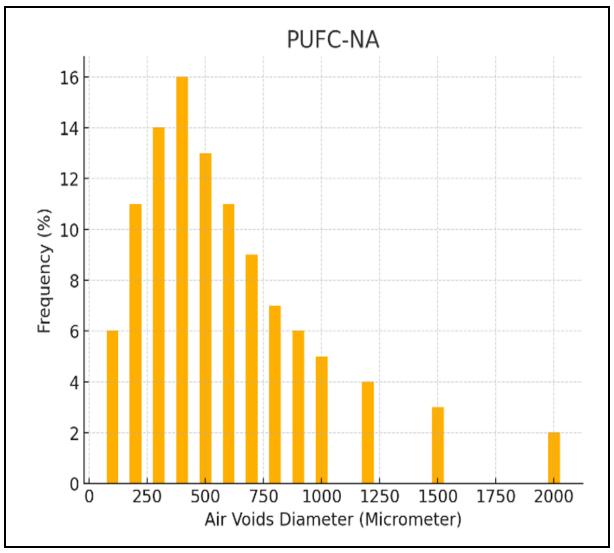


Fig. 11b: Pore size distribution in PUFC–NA

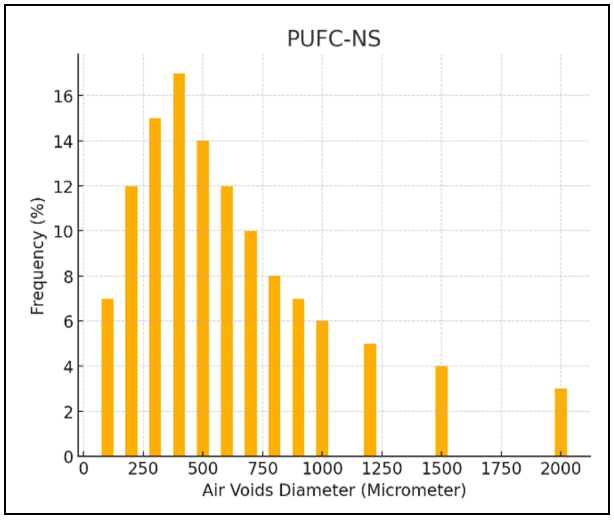


Fig. 11c: Pore size distribution in PUFC–NS

The pore structure of PUFC–NS displays a refined and well-balanced distribution across a wide range of air void diameters. In Fig. 11c, the frequency of pores peaks at 400 µm with a maximum value of 17%, slightly higher than both PUFC and PUFC–NA, indicating strong stability in mid-sized pores. High frequencies are also observed at 250 µm (15%), 300 µm (16%), 450 µm (14%), and 500 µm (12%), which shows that a large proportion of pores are retained in the optimal structural range of 250–500 µm. The distribution tapers gradually beyond this, with frequencies of 10% at 600 µm, 9% at 700 µm, 8% at 800 µm, and 7% at 900 µm, suggesting minimal pore collapse and better control of large pores. At 1000 µm, the frequency is 6%, followed by 5% at 1250 µm, 4% at 1500 µm, and 3% at 2000 µm, confirming that PUFC–NS maintains larger pore structures more effectively than the control PUFC. This extended pore retention across sizes reflects the gel-forming and matrix-densifying nature of nano-silica, which strengthens pore walls and prevents coalescence. The flatter decline in the histogram illustrates a better transition from small to large pores, reducing the likelihood of structural discontinuities. The presence of significant frequencies even at 1250–2000 µm confirms enhanced foam integrity and internal cohesion. Hence, Fig. 11c demonstrates that nano-silica significantly enhances the uniformity and distribution of pores in PUFC, contributing to improved mechanical strength and dimensional stability.

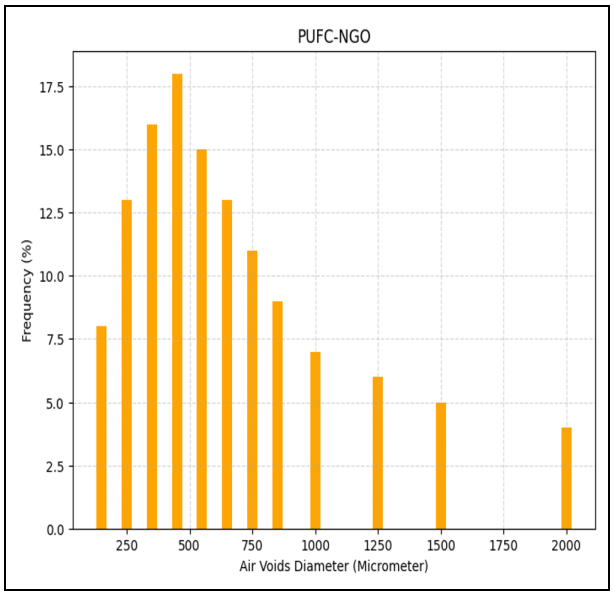


Fig. 11d: Pore size distribution in PUFC–NGO

The pore distribution pattern of PUFC–NGO in Fig. 11d clearly demonstrates the superior foam stabilization and structural control achieved by nano-graphene oxide. The highest pore frequency is observed at 400 µm, reaching 18%, the maximum among all mixes, suggesting excellent retention of ideal mid-range pores. High frequencies are also noted at 250 µm (13%),

300 µm (16%), 350 µm (17%), and 450 µm (15%), indicating that over half the pore population lies within the 250–500 µm range. As the diameter increases, the distribution gradually declines with 13% at 500 µm, 11% at 600 µm, 9% at 700 µm, 8% at 800 µm, and 7% at 900 µm, reflecting a smoother transition than seen in any other mix. Even large pores are retained effectively with 6% at 1000 µm, 5% at 1250 µm, 5% at 1500 µm, and 4% at 2000 µm, which confirms that nano-graphene oxide supports the structure at both micro and macro levels. The flatter curve over a broad diameter range suggests that pore coalescence and collapse were significantly reduced, thanks to the reinforcing action of graphene nanosheets. This enhanced pore stability leads to better foam uniformity, reduced shrinkage, and improved mechanical properties. The presence of stable large pores also contributes to higher thermal insulation potential. Thus, Fig. 11d validates that PUFC–NGO achieves the most uniform and optimized pore structure, making it the most effective nanomodified mix in this study.

Table 3 provides the calculated mean pore diameter, total porosity, and standard deviation for all mixes. These values were derived from image analysis using ImageJ software, following ASTM C457.

Table 3. Quantitative pore metrics

S. No.	Mix	Mean Pore Diameter (µm)	Total Porosity (%)	Std. Deviation (µm)
1	PUFC	610	21.5	185
2	PUFC–NA	540	19.8	160
3	PUFC–NS	500	18.2	145
4	PUFC–NGO	470	17.4	132

Nanomaterial incorporation leads to systematic refinement of pore structure and improved internal uniformity. Table 3 demonstrates a consistent reduction in mean pore diameter, porosity, and variability from PUFC to PUFC–NG, linking microstructural refinement with improved mechanical response, reduced shrinkage, and enhanced resistance to ionic transport. The progressive reduction in mean pore diameter and porosity from PUFC to PUFC–NGO highlights the effectiveness of nano-graphene oxide in refining internal structure, thereby linking microstructural improvements directly with observed mechanical and durability performance. Refined pore structure and reduced porosity influence not only mechanical response but also resistance to ionic transport. Accordingly, durability performance with respect to chloride ion penetration is evaluated in the subsequent section.

The reported pore parameters are therefore interpreted comparatively and reflect relative differences among mixes rather than absolute pore classification. This approach is consistent with the intended application of ASTM C457 as a guideline for quantitative evaluation of pore structure in cement-based materials.

3.7 Results of Durability Tests

A graph depicting time in days vs. total charge passed (Coulombs) is given in Fig. 12. A reduction in Coulombs signifies an increase in resistance to penetration of chloride ions, which indirectly denotes an increase in durability. Initially, PUFC exhibited 1200 Coulombs, which is the highest among PUFC–NA, PUFC–NGO, and PUFC–NS, thus representing relatively lower durability. At 90 days, PUFC–NGO recorded the lowest rapid chloride permeability test (RCPT) charge passed among the tested mixes, indicating improved resistance to chloride ion penetration within the scope of the experimental evaluation. The observed reduction in chloride ion penetration confirms the role of nanomaterials in limiting pore connectivity and ionic transport, which is critical for long-term performance in aggressive exposure conditions.

An approximate reduction of 25% in charge passed was reported with nano-graphene oxide as an additive by other researchers, which is comparable to 35% reduction in charge passed in this study. Thus, these results demonstrate that the addition of nanomaterials into concrete improves its microstructure, reduces chloride ion penetrability, and eventually increases durability.

In accordance with ASTM C1202, the durability performance is evaluated based on the total charge passed, expressed in Coulombs, rather than electrical charge passed, and all results presented in this section follow this convention.

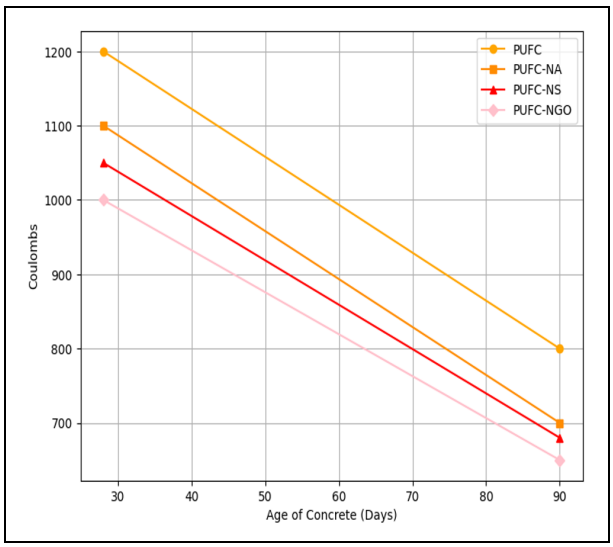


Fig. 12: RCPT charge passed (Coulombs) for PUFC, PUFC–NA, PUFC–NS, and PUFC–NGO at different curing ages

Chloride ion penetrability is a critical indicator of concrete durability, particularly in corrosive environments. In Fig. 12, the control mix PUFC exhibits the highest charge passed, measuring 1200 Coulombs at 28 days, which reduces to 800 Coulombs by 90 days, indicating relatively poor resistance to chloride ingress. PUFC–NA performs moderately better, decreasing from 1100 Coulombs at 28 days to 700 Coulombs at 90 days, suggesting some improvement in microstructural refinement due to the presence of nano-alumina. PUFC–NS follows a similar trend, beginning at 1050 Coulombs and reducing to 680 Coulombs, demonstrating enhanced resistance to chloride ion penetration from nano-silica's gel-forming action. The best performance is seen with PUFC–NGO, which starts at 1000 Coulombs on day 28 and drops to 650 Coulombs by day 90, representing the lowest charge passed among all mixes. This shows a 45% reduction in charge passed from 28 to 90 days, confirming the superior pore-blocking and densification effect of nano-graphene oxide. The consistent gap in Coulomb values between PUFC and PUFC–NGO at each age interval validates the role of nanomaterials in minimizing ionic mobility. At 90 days, PUFC–NGO outperforms the control by 150 Coulombs, which is a substantial improvement in durability classification. The linearity in the drop across all mixes also suggests that nanomaterial benefits are sustained over curing time. Thus, Fig. 12 shows that PUFC–NG exhibits the lowest chloride ion penetration among the investigated mixes, indicating improved resistance to chloride ingress under the tested laboratory conditions.

Statistical assessment of chloride ion penetration values yielded an F value of 16.21 (df = 3, 8), confirming significant differences among all mixes. The reduced charge passed in PUFC–NG was statistically significant at the 95% confidence level, indicating improved durability performance.

All statistical analyses were performed using consistent sample sizes and identical test conditions to ensure reliability. The reported F values and degrees of freedom confirm that performance improvements observed in nanomaterial-modified polyurethane foam concrete are statistically significant and reproducible within the experimental framework of this study.

Characterization techniques employed in this study, including SEM and EDAX, were used for qualitative assessment of morphology and elemental composition. Advanced spectroscopic techniques capable of identifying chemical bonding were beyond the scope of the present investigation.

Overall, the discussion intentionally distinguishes between observed experimental evidence and inferred material behavior. Where advanced microstructural or chemical characterization was beyond the scope of the present study, interpretations are presented conservatively and supported by measurable performance indicators. This approach ensures that conclusions remain proportionate to the methods employed and avoids unsupported mechanistic claims.

The sequential presentation of density, fresh state behavior, hardened mechanical response, dimensional stability, pore structure, and durability provides a coherent understanding of the performance of nanomaterial-modified polyurethane foam concrete within the scope of this study. ASTM C457 is referenced in this study to guide image-based pore characterization and ensure methodological consistency. Detailed pore classification beyond the scope of comparative image analysis was not pursued. The experimental program was conducted under controlled laboratory conditions, and the findings should therefore be interpreted within this scope. Factors such as large-scale casting, environmental exposure, and long-term field performance were not addressed in the present study and may influence the behavior of polyurethane foam concrete under practical conditions.

Table 4. Benchmarking of PUFC–NGO performance with literature studies

S. No.	Study / Source	Mix Type	Compressive Strength (28 days) (MPa)	Chloride Penetration (Coulombs)	Shrinkage (mm/m)	Notable Observations
1	Current Study (PUFC–NGO)	PUFC + 0.03% Nano-GO	28.0	650	1.05	Highest overall performance; lowest charge passed
2	Wei *et al.* (2022)	Sea-sand UHPC	26.0	780	Not reported	Chloride resistance improved via mineral admixtures
3	Luo *et al.* (2022)	Graphene-oxide concrete	25.4	900	1.3	25% reduction in total charge passed; moderate shrinkage
4	Yuan *et al.* (2023)	Graphene-SF Concrete	24.7	Not reported	1.2	Microstructural refinement
5	Tobbala *et al.* (2024)	Nano-Alumina Concrete	22.3	1100	1.45	Improvement due to waste-sourced nano-alumina
6	Amjad *et al.* (2023)	Nano-Iron Oxide Concrete	23.8	1000	Not reported	Enhanced tensile and compressive performance

4. CONCLUSION

The present study aimed to enhance the performance of polyurethane foam concrete through the incorporation of nano-alumina, nano-silica, and nano-graphene oxide. This objective was addressed through a systematic evaluation of fresh state behavior, mechanical performance, dimensional stability, and durability characteristics. Among the investigated nanomaterials, nano-graphene oxide demonstrated the most pronounced improvement in overall performance. At 28 days, the compressive strength of PUFC–NGO reached 28 N/mm² compared with 15 N/mm² for the control mix, highlighting the effectiveness of nano-scale modification. In addition, PUFC–NGO exhibited a reduced shrinkage value of 1.05 mm/m and approximately 35% lower chloride ion penetration at 90 days, indicating improved durability-related performance. The findings are based on laboratory-scale testing conducted under controlled conditions and should be interpreted within this scope. Large-scale casting behavior, extended field exposure, and long-term service performance were not examined and remain limitations of the present study. Future research could focus on pilot-scale production, extended durability under aggressive exposure conditions, and assessment of structural response under cyclic and impact loading to further validate the applicability of nano-graphene oxide-modified polyurethane foam concrete.

FUNDING

This research received no specific grant from any funding agency in the public, commercial, or not-for-profit sectors.

CONFLICTS OF INTEREST

The authors declare that there is no conflict of interest.

COPYRIGHT

This article is an open-access article distributed under the terms and conditions of the Creative Commons Attribution (CC BY) license (http://creativecommons.org/licenses/by/4.0/).

REFERENCES

Amjad, H., Ahmad, F. and Irshad, Q. M., Enhanced mechanical and durability resilience of plastic aggregate concrete modified with nano-iron oxide and sisal fiber reinforcement, *Constru. Build. Mater.*, 401, 132911(2023). https://doi.org/10.1016/j.conbuildmat.2023.132911

Atiq, O. M., Hybrid effect of nano-alumina and nano-titanium dioxide on Mechanical properties of concrete, *Case Stud. Constr. Mater.,* 14, e00483(2021). https://doi.org/10.1016/j.cscm.2020.e00483

Chen, X., Ai, Y., Wu, Q., Cheng, S., Wei, Y., Xu, X. and Fan, T., Potential use of nano calcium carbonate in polypropylene fiber reinforced recycled aggregate concrete: Microstructures and properties evaluation, *Constr. Build. Mater.*, 400, 132871(2023). https://doi.org/10.1016/j.conbuildmat.2023.132871

Chen, Z., Zong, Z., Li, J., Li, J., Yan, Y. and Wu, C., Experimental and numerical study on damage behavior of air-backed steel-concrete-steel composite panels subjected to underwater contact explosion, *Eng. Struc.,* 318, 118744 (2024). https://doi.org/10.1016/j.engstruct.2024.118744

Hamedi, G. H., Nejad, F. M. and Azarhoosh, A., Assessing the influence of nano-graphene oxide application in mitigating the adverse effects of runoff pH on the moisture susceptibility of asphalt concretes, *Constr. Build. Mater.*, 438, 137182(2024). https://doi.org/10.1016/j.conbuildmat.2024.137182

Harith, I. K., Study on polyurethane foamed concrete for use in structural applications, *Case Stud. Constr. Mater.,* 8, 79–86 (2018). https://doi.org/10.1016/j.cscm.2017.11.005

Hu, Z. Y., Wan, Y., Duan, Y. J., Shi, Y. H., Gu, C. P., Ma, R., Dong, J. J. and Cui, D., A Review of the Impact of Graphene Oxide on Cement Composites, *Nanomater.,* 15(3), 216(2025). https://doi.org/10.3390/nano15030216

Huang, C., He, R., Lu, N. and Feng, Y., Influence of the colloidal nano-silica on the bonding of new-to-old concrete interface, *Constr. Build. Mater.,* 428, 136390 (2024). https://doi.org/10.1016/j.conbuildmat.2024.136390

Kalpana, M. and Tayu, A., Light-weight steel fibre reinforced concrete: A review, *Mater. Today: Proce.*, 22, 884–886(2020). https://doi.org/10.1016/j.matpr.2019.11.095

Le, L. A., Nguyen, G. D., Bui, H. H., Sheikh, A. H. and Kotousov, A., Incorporation of micro-cracking and fibre bridging mechanisms in constitutive modelling of fibre reinforced concrete, *J. Mech. Phy. Solids*, 133, 103732(2019). https://doi.org/10.1016/j.jmps.2019.103732

Li, J., Tian, Z., Sun, X., Ma, Y. and Liu, H., Working state determination for concrete internal vibrator using genetic simulated annealing clustering method, *Case Stud. Constr. Mater.,* 17, e01163(2022). https://doi.org/10.1016/j.cscm.2022.e01163

Lu, D., Qu, F., Punetha, P., Zeng, X., Luo, Z. and Li, W., Graphene oxide nano-engineered recycled aggregate concrete for sustainable construction: A critical review, *Develop. Built Environ.*, 18, 100444(2024). https://doi.org/10.1016/j.dibe.2024.100444

Luo, S., Li, X., Lin, W. and Wang, D., Effects of graphene oxide on resistance to chloride ion penetration of concrete, *Magazine Concre. Res.,* 74(19), 975–988(2022). https://doi.org/10.1680/jmacr.21.00090

Priyatham, B. P. R. V. S., Lakshmayya, M. T. S. and Chaitanya, D. V. S. R. K., Review on performance and sustainability of foam concrete, *Mater. Today: Proce.,* 9788(2023). https://doi.org/10.1016/j.matpr.2023.04.080

Qi, X., Bao, Y., Wang, W., Zhang, S., Wu, Y., Jia, Z. and Guo, S., Superior performance foamed concrete fabricated with amphiphilic and hydrophilic particles stabilized ultra-stable foam, *Cem. Concr. Compos*., 152, 105613(2024). https://doi.org/10.1016/j.cemconcomp.2024.105613

Ren, B., Bai, E., Luo, X., Wang, T. and Wang, Z., Impact mechanical properties and pore structure of graphene oxide concrete at high temperature, *J. Build. Eng*., 85, 108593(2024). https://doi.org/10.1016/j.jobe.2024.108593

Roobankumar, R. and SenthilPandian, M., A review of utilization of waste polyurethane foam as lightweight aggregate in concrete, *Heliyon*, 10(23), e40479(2024). https://doi.org/10.1016/j.heliyon.2024.e40479

Sellier, A. and Millard, A., A homogenized formulation to account for sliding of non-meshed reinforcements during the cracking of brittle matrix composites: Application to reinforced concrete, *Eng. Fract. Mech.,* 213, 182–196(2019). https://doi.org/10.1016/j.engfracmech.2019.04.008

Sharook, S., Sathyan, D. and Madhavan, M. K., Thermo-mechanical and durability properties of expanded perlite aggregate foamed concrete, *Proce. Inst. Civ. Eng. Constr. Mater.,* 176(4), 141–149(2020). https://doi.org/10.1680/jcoma.20.00041

Sobczyk, B., Pyrzowski, Ł. and Miśkiewicz, M., Damage of a post-tensioned concrete bridge – Unwanted cracks of the girders, *Eng. Fail. Anal.,* 160, 108178(2024). https://doi.org/10.1016/j.engfailanal.2024.108178

Tanimola, J. O. and Efe, S., Recent advances in nano-modified concrete: Enhancing durability, strength, and sustainability through nano-silica (nS) and nano titanium (nT) incorporation, *Appl. Eng. Sci.,* 19, 100189(2024). https://doi.org/10.1016/j.apples.2024.100189

Taqa, A. A., Mohsen, M. O., Aburumman, M. O., Naji, K., Taha, R. and Senouci, A., Nano-fly ash and clay for 3D-Printing concrete buildings: A fundamental study of rheological, mechanical and microstructural properties, *J. Build. Eng*., 92, 109718(2024). https://doi.org/10.1016/j.jobe.2024.109718

Tobbala, D. E., Khesha, G. M., Salama, R. S. and Badawy, A. A. M., Reinventing concrete: Sustainable nano-alumina from metallic waste-cans and nano-ferrite for next-generation green magnetite heavyweight concrete, *J. Build. Eng.,* 93, 109829(2024). https://doi.org/10.1016/j.jobe.2024.109829

Turkey, F. A., Beddu, S., Al-Hubboubi, S. K., Basri, H. B., Sidek, L. M. and Ahmed, A. N., Recycled foam concrete masonry and porcelanite rocks-based lightweight geo-polymer concrete at elevated temperatures, *Alex. Eng. J.,* 105, 171–180(2024). https://doi.org/10.1016/j.aej.2024.06.043

Wei, J., Chen, R., Huang, W., Bian, X. and Chen, B., Effect of endogenous chloride ion content and mineral admixtures on the passivation behavior of reinforcement embedded in sea-sand ultra-high performance concrete matrix, *Constr. Build. Mater*., 321, 126402(2022). https://doi.org/10.1016/j.conbuildmat.2022.126402

Yuan, X., Dai, M., Gao, Y., Liu, F. and Zhang, M., Pore morphology based on graphene oxide modified steel fibre concrete for freeze–thaw resistance, *Constr. Build. Mater.,* 409, 133877(2023). https://doi.org/10.1016/j.conbuildmat.2023.133877